Removal of Cu^{2+} from wastewater by modified Xanthan gum (XG) with ethylenediamine (EDA)

Hanyan Qiu1,2, Junhua Yan2, Guihong Lan1,2*, Yongqiang Liu3, Xiaoqin Song1, Wanxi Peng1 and Yingyi Cui1

1 State Key Laboratory of Oil Gas Reservoir Geology and Exploitation, Southwest Petroleum University, Chengdu 610500, China.

2 College of Chemistry and Chemical Engineering, Southwest Petroleum University, Chengdu 610500, China.

3 Faculty of Engineering and the Environment, University of Southampton, Southampton SO171BJ, United Kingdom.

*Corresponding author. E-mail: guihonglan416@sina.com

ABSTRACT:

Herein, a new adsorbent was synthesized by modifying xanthan gum for the removal of Cu^{2+} fromwastewater. Xanthan gum was first successfully modified with thionyl chloride followed byethylenediamine. The modified xanthan gum was characterized via Fourier transform infraredspectrometry (FTIR), carbon nuclear magnetic resonance (^{13}C NMR), scanning electron microscopy (SEM),energy dispersion spectroscopy (EDS) and thermogravimetry (TG) for a better understanding of its Cu^{2+}removal efficiency. In addition, the effects of pH, contact time, adsorbent dosage, initial concentration ofCu^{2+} and coexisting ions on the adsorption of Cu^{2+} were investigated via batch adsorption studies. Results suggest that the adsorption process of Cu^{2+} follows a pseudo second order kinetics model withan equilibrium time of 120 min. The experimental data could be fitted with the Langmuir isotherm better than the Freundlich model. The adsorption capacity of Cu^{2+} by the modified xanthan gum reached up to46.95 (mg g_1). The adsorbent could be easily regenerated by only the addition of 0.1 M HCl. Also, theadsorption effect of other divalent cations by XG-NH_2 was preliminarily investigated.

Keywords: ethylenediamine; xanthan gum; adsorption; copper ions

Introduction

With continuous development in industrialization, industrial wastewater containing a large amount of heavy metals demands great attention for efficient and economical treatment. Copper is regarded as one of the most important and hazardous inorganic contaminants in the environment. After being discharged into an area with biological activity, copper is apt to accumulate in organisms and steadily exist in the biosphere. Meanwhile, since copper is non-biodegradable and toxic, it easily causes serious harm to the entire ecosystem through the food chain. Moreover, on account of the diverse application of copper, copper is considerably produced from wide sources such as mining, electroplating, metal processing, petroleum refining, paints and pigments, paper and pulp, steel-works, and pesticides containing Cu.1–4 To reduce the hazards caused by copper, several technologies have been developed to remove Cu2+ such as chemical precipitation, filtration and coagulation, exchange, chemical reduction, membrane separation, biological treatment, solid phase extraction, and adsorption.5–7 Among these methods, adsorption is considered as one of the most cost-effective and efficient alternative, which has resulted in a lot of research in this area recently. Till date, a large number of adsorbents have been employed to treat effluents containing copper ions by providing chemical active sites or various functional groups including carboxyl, amide and hydroxyl groups, such as sugar-beet pulp pectin gels,8 cellulosic-adsorbent resins,9 and orange peel.10 In addition, to enhance the adsorption capacity of

heavy metals, different types of functional groups have been introduced into raw adsorbent materials. T. S. Anirudhan et al.11 found that the binding capacity of chitosan for Cu evidently increased by synthesizing glutaraldehyde crosslinked epoxyaminated chitosan due to the introduction of abundant amide and hydroxyl groups. E. Pehlivan et al.12 synthesized a potential bio-sorbent by modifying barley straw with citric acid, which resulted in a significant increase in the uptake amount of copper because of the enhanced chelation of copper with sufficient carboxyl groups from citric acid.

Xanthan gum (XG) is as an anionic extracellular heteropolysaccharide obtained from corn, which is mainly produced by Xanthomonas campestris through fermentation under aerobic conditions.13,14 It is a polymer with a high-molecular weight of approximately 106 to 107 DA, and consists of b-(1-4)-D-glucopyranose units with plentiful acetic and pyruvic moieties,15 which is similar to cellulose. Thus, far considerable attention has been paid to XG. It is widely being used in bio-medicine,16 O/W emulsions,17 and food and tissue engineering.18 In recentyears, XG has been studied for the removal of heavy metals from wastewater due to its chemical structure with abundant hydroxyl and carboxyl groups which possess excellent adsorption properties by chelation between functional groups and heavy metals.19–21 Due to the fact that natural XG dissolves easily in water at ambient temperature, it is difficult to separate it from water after adsorption of heavy metal ions. Thus, the direct application of XG for heavy metal removal from wastewater is highly restricted. Hence, the modification of absorbents by introducing functional groups or combining with inorganic compounds is promising for real applications to overcome this limitation. Furthermore, more hydroxyl, carboxyl and amino groups mean a higher adsorption capacity of heavy metals.

At present, the chemical modification of bio-polymers, depending on the active functional groups of the original material, is one of the most common and effective methods to introduce new active functional groups for cation removal from wastewater.22–24 After completion of the modification reaction, the chemical and physical properties of these materials are also changed because of the new functional groups on their surfaces. In recent years, some studies have reported successful modification methods for cellulose due to the available hydroxyl groups, in which the chlorine atom is usually applied to generate halogen derivatives and then corresponding chelating groups are introduced by nucleophilic substitution.25,26 Similar to cellulose, a large number of polysaccharide materials that are widely present in nature contain massive hydroxyl groups, which are the most reactive positions in the modification process.27 Therefore, it is easy to modify this type of material by utilizing hydroxyl groups.

In this study, we synthesize a novel adsorbent using ethylenediamine to modify soluble XG, which is able to overcome the constraints of original XG for wastewater treatment. The modified XG was used to remove Cu2+ ions and the operational conditions for Cu2+ adsorption were studied. Furthermore, adsorption isotherms and kinetics models were investigated to explore the possible adsorption mechanism. Finally, desorption experiments were also conducted to evaluate the regeneration performance of the modified XG. In addition, the adsorption effect of different divalent cations was also preliminarily studied.

2. Experimental

2.1 Materials

Xanthan gum (XG), thionyl chloride (SOCl2), N0,N-dimethylformamide (DMF), ammonium hydroxide, ethylenediamine (EDA) and ethanol of analytical grade were purchased from the Kelong Chemical Reagent Factory, Chengdu, China. Distilled water was used in all experiments.

2.2 Preparation of XG-NH_2 adsorbent

Referring to the literature on modified cellulose using ethylenediamine, 25,27,28 the xanthan gum-based heavy metal adsorption material (XG-NH2) was prepared as follows: 10.0 g XG waspreviously heated at 323 K for 24 h to activate XG and then suspended in 200 mL DMF, followed by slow addition of 35 mL thionyl chloride (SOCl2) with continuous mechanical stirring at 353 K. The product from the reaction after stirring for 4 h at 353 K was washed with several aliquots of diluted ammonium hydroxide, and then filtered. The suspension was washed with distilled water until the pH was neutral. The final solid (XG-Cl) was filtered and dried overnight at 323 K in a drying oven.

To obtain XG-NH2, 2.0 g XG-Cl was added to a 3 mouth flask with 40 mL distilled water, and was heated to 353 K in a submersible stirrer, followed by the addition of 30 mL ethylenediamine. The mixture was refuxed with magnetic stirring for 3 h at 353 K. After the reaction was complete, the mixture was cooled to room temperature and precipitated with a certain amount of ethanol. The solid obtained, was washed with distilled water until it approached to a neutral pH and was centrifuged. Finally, the solid XG-NH2 was dried at 323 K for 24 h, and ground for the next application. The solubility of XG-NH2 as determined by a gravimetric method at 35 _C is 0.0081 g/100 g H2O. Meanwhile, the chemical synthetic scheme of XG-NH2 is illustrated in Fig. 1.

2.3 Characterization of XG-NH_2

In order to study the binding functional groups of the modified XG with Cu ions, the dried adsorbent was characterized by Fourier transform infrared spectrometry (FTIR) on a WOF-520 spectrometer using KBr pellets. In addition, the modified XG was further analyzed via carbon nuclear magnetic resonance (13C NMR, Bruker AVANCE III) in the solid state. Themorphology and size of the adsorbent XG-NH2 was characterized via scanning electron microscopy (SEM, JSM-7500F) analysis at 10.0 kV. The sample element composition and contents were analyzed by energy dispersive spectroscopy (EDS) coupled to SEM. Thermal gravity analysis/differential thermal gravity (TG/DTG) analyses were determined under air atmosphere on a TG (NETZSCH STA 449F3) instrument scanned from 40 to 800 _C.

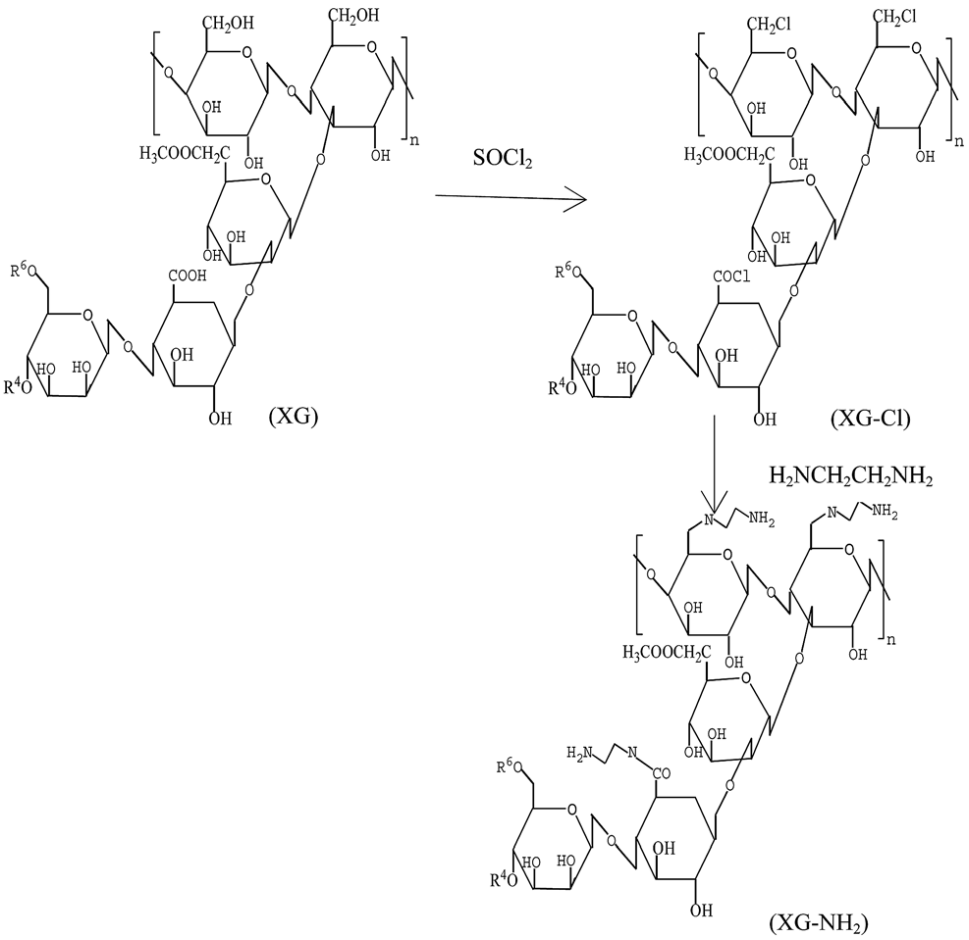

Fig 1 Chemical synthetic scheme of XG-NH_2

2.4 Adsorption experiments

Batch adsorption experiments were carried out in a constant temperature shaker (QYC-200, Chengdu, China) at 30 _C for 2 h at 250 rpm. Adsorption experiments were performed by adding a certain amount of XG-NH2 to a 50 mL Cu2+ solution in a 250 mL conical flask at different concentrations of Cu2+ and different pH. After the adsorption reaction was completed, the solution was centrifuged for 3 min at 3000 rpm to separate the adsorbent. Finally, the initial and final concentrations of Cu2+ solution were measured via atomic adsorption spectrophotometry (AA-7020, Beijing, China).

To optimize the experimental conditions, the effect of pH on adsorption capacity was determined by mixing 0.1 g XG-NH2 with 50 mL Cu2+ (100 mg L_1) in a 250 mL conical flask in a constant temperature shaker at 30 _C for 2 h at 250 rpm. The pH value was adjusted with 1 M hydrochloric acid or 1 M sodium hydroxide ranging from 2 to 6. To study the effect of XGNH2 dosage on adsorption capacity, different amounts of the adsorbent were mixed with 50 mL Cu2+ (100 mg L_1) solutions at pH 5.0 _ 0.1 in 250 mL conical flasks in a constant temperature shaker at 30 _C at 250 rpm. After 2 h, the final centrifuged supernatants were measured. To investigate adsorption kinetics, the contact time was varied from 10 to 180 min and kinetics experiments were performed using 150 mL Cu2+ (100 mg L_1) solutions with a 0.3 g XG-NH2 dose. Different solutions were withdrawn to analyze the changes in concentration at different time intervals. Isotherms were obtained for various initial concentrations ranging from 69 to 885 mg L_1 with a 0.1 g adsorbent dose. The effects of coexisting ions on adsorption were investigated by adding different types of salts to solutions containing 100 mg L_1 Cu2+ and the adsorption capacity of Cu2+ was calculated. In addition, to further study the adsorption

capacity of different divalent cations by XG-NH2, different adsorption experiments were conducted by mixing 0.1 g XGNH2 with 50 mL of 100 mg L_1 different divalent cations. All adsorption experiments were carried out in triplicate.

The adsorption capacity (qe) of the adsorption was calculated using the following equation:

$$q = \frac{(C_0 - C_e)V}{m} \quad (1)$$

where, (qe) is the equilibrium adsorption capacity (mg g_1), and C0 and Ce are the initial and equilibrium concentration (mg L_1), respectively. m is the mass of adsorbent (g) and V is the volume of Cu2+ solution (mL).

2.5 Desorption studies

To effectively reuse the adsorbent, batch desorption experiments were conducted to study the recycle times of XG-NH2. Thus, far, some regents have been employed to regenerate adsorbents, e.g. HCl, NaOH, HNO3, EDTA.3,29,30 In this paper, HCl has been chosen as the regeneration regent. 0.5 g adsorbents loaded by Cu2+ were soaked in 25 mL of 0.1 M HCl and shaken for 2 h at 250 rpm at 30 _C. The adsorbents were recycled four times to evaluate the regeneration capability of adsorbent.

3. Results and discussion

3.1 Characterization

The FTIR spectra of xanthan gum and its modi ed bio-polymers are shown in Fig. 2. Fig. 2a shows the characteristic absorption peaks of xanthan gum, which are highly consistent with the reports from the literature.31,32 The strong band at 3407 cm_1 denotes the typical stretching vibration for the –OH group. The band for the methyl group appeared at 2918 cm_1. The two bands at 1621 cm_1 and 1405 cm_1 represent stretching of the carbonyl (C]O) ester of the acetyl groups and asymmetrical stretching of C]O for the carboxyl group. The C–O of the primary alcohols caused the stretching vibration at 1052 cm_1. From Fig. 2b, it can be seen that the changes in the adsorption peaks of xanthan gum modified with thionyl chloride are prominent. The displacement of the peak at 1049 cm_1 is attributed to the sulfoxide group (S]O). Also, the appearance of a new band at 1725 cm_1 is the stretching of the acyl chloride group, which is ascribed to the substitution of the hydroxyl group from the carboxyl group by chlorine atoms. Compared with the band of xanthan gum at 3407 cm_1, there are some new peaks in Fig. 2b, which reveal the successful displacement of the hydroxyl group by chlorine atoms. Furthermore, there were major shifts in Fig. 2c, in which the sharp peaks at 1113 cm_1 and 1028 cm_1 indicate the further reaction of modified xanthan gum by thionyl chloride with ethylenediamine. The bands at 1405 cm_1 and 1621 cm_1 are attributed to –CN stretching and –NH2 (amide II) stretching, respectively. The broad peak at 3407 cm_1 corresponds to the overlapping of asymmetrical OH and NH stretches. After Cu2+ uptake in XG-NH2, as shown in Fig. 2d, the two peaks at 1113 cm_1 and 1028 cm_1 of XG-NH2 merge into one peak at 1038 cm_1, which shows the success of Cu2+ adsorption. Meanwhile, the broadened peak at 1621 cm_1 can be explained by the chelation of Cu2+ and –NH2. A new peak appeared at 3125 cm_1 and the peak at around 3425 cm_1significantly weakened, which might be due to the hydrogen bond and chelation between Cu2+ and –OH.

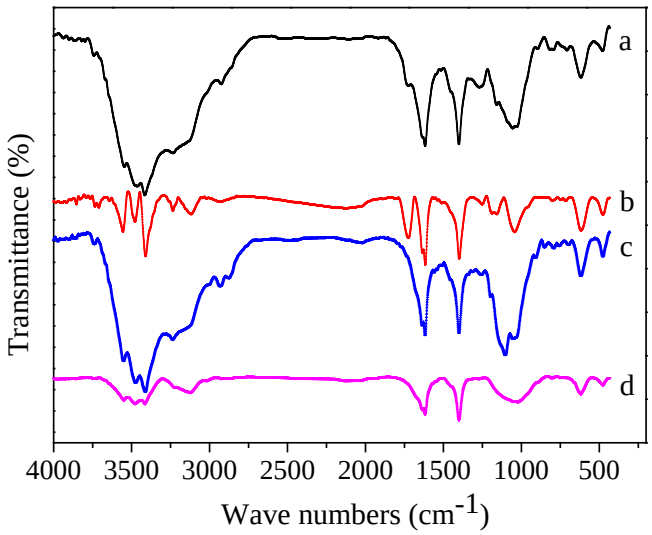

Fig 2 FTIR spectrum of XG (a), XG-Cl (b), XG-NH_2 (c) and XG-NH_2 loaded by Cu^{2+}(d).

Fig. 3 shows the 13C NMR of XG-NH2 in the solid state. As shown in Fig. 3, the weak peak at 172 ppm is ascribed to –CONH2. Moreover, it can be evidently observed that peaks appeared at 102 ppm, 73 ppm and 39 ppm. The peaks at 73 ppm and 39 ppm could be due to the –C–N groups. These results are in agreement with the FTIR results, which indicate that –NH2 groups were successfully introduced. Fig. 4 displays photographs of XG-NH2 before and after adsorption of Cu2+, which reveals the dramatic color change of the adsorbent after reacting with a Cu2+ solution. Moreover, the SEM micrographs of XG and its modified polymers are shown in ESI Fig. S1.† As shown in Fig. S1a,† the morphology of XG is granular.19 After chlorination, the granular appearance of XG changed to a fibrillar structure. After the material was further reacted with ethylenediamine, the fibrillar structure of XG-Cl (Fig. S1b†) disappeared and a smooth small surface was achieved.

Compared with Fig. S1c,† the microtopography (Fig. S1d†) of loaded Cu on XG-NH2 is more smooth and coherent. Fig. 5 shows the EDS spectra of XG (Fig. 5a), the chlorination of xanthan gum (Fig. 5b), and XG-NH2 before (Fig. 5c) and after (Fig. 5d) adsorption of Cu2+. Fig. 5a is the EDS spectrum of the unmodified XG, in which C, O, Ca and Cl elements were detected. Compared with Fig. 5a, an S peak was obtained and the Cl and C peak strength increased prominently in Fig. 5b, which indicate the successful modification with thionyl chloride. Due to the limitation of the EDS analysis of the N element, there was no N detected in Fig. 5c after the use of ethylenediamine for further modification. However, the increase in the C peak and decrease in the S and Cl peaks reveal the success of the further modification with ethylenediamine. In Fig. 5d, the appearance of Cu element further confirms the successful adsorption of Cu2+ on XG-NH2.

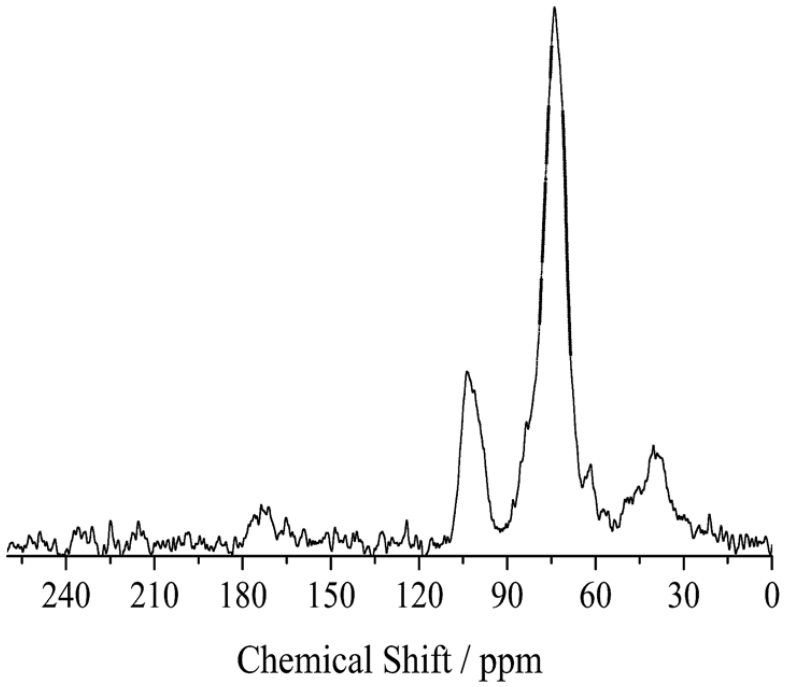

Fig. 3 Solid state $_{13}$C NMR of XG-NH_2.

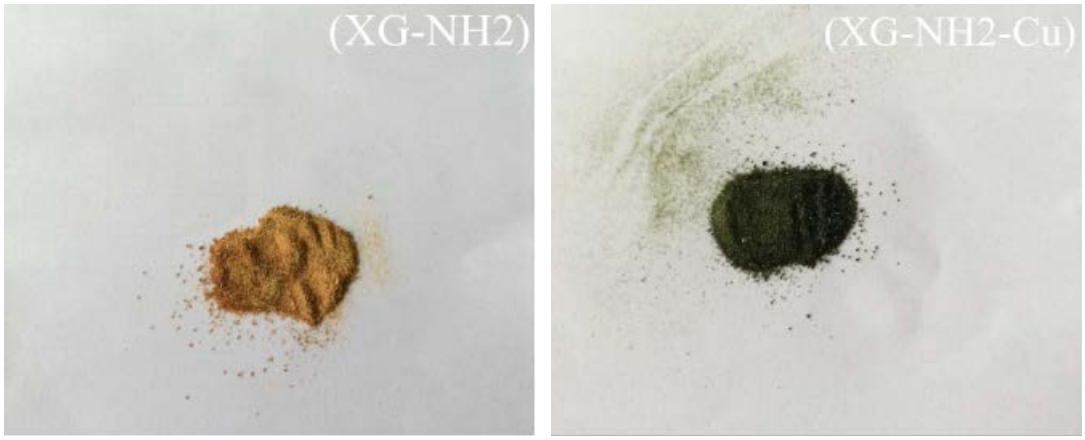

Fig 4 the photographs of XG-NH_2 and XG-NH_2 loaded by Cu^{2+}

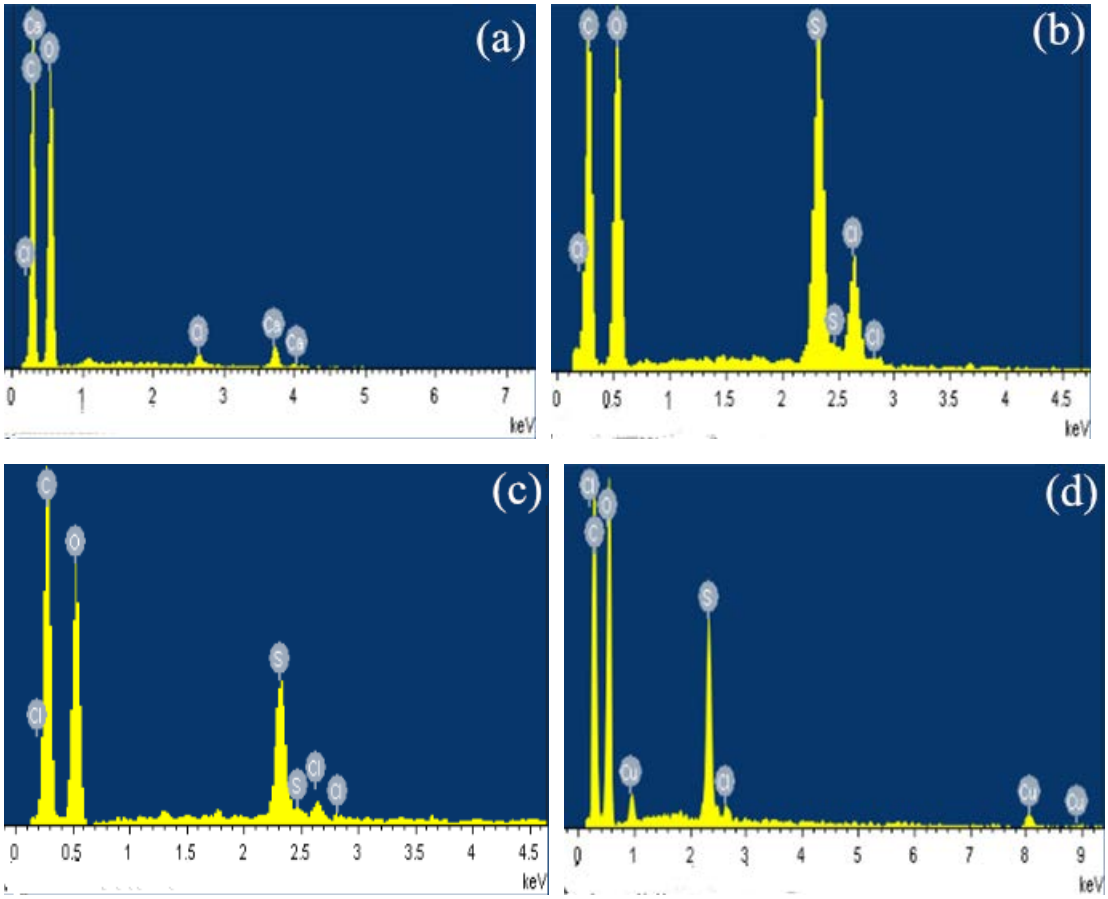

Fig 5 EDS spectrum of of XG(a), XG-Cl(b), XG-NH2(c) and XG-NH2 loaded by Cu2+(d).

The TG/DTG curves of XG and modi ed XG are shown in Fig. 6. As shown in Fig. 6, when the temperature was below 200 _C, there was mass loss for the three samples, which is attributed to the loss of free water as well as bound water. The DTG curve of XG displays a degradation temperature at 288 _C, which is possibly due to polysaccharide degradation.32,33 Comparing XG with XG-NH2 and XG-Cl in the 200 to 383 _C range, it can be clearly seen that the decomposition temperature of XG is higher, which proves the success of modification. With regard to XG-Cl and XG-NH2, the corresponding degradation temperatures were 257 _C and 272 _C, respectively, which are ascribed to the loss of hydrogen chloride and ammonia together with polysaccharide degradation.25,32 In addition, imide groups were formed with the loss of ammonia from XGNH2.34 The further mass loss from 383 _C to 578 _C for XG and XG-Cl is assigned to the further pyrolytic decomposition of polysaccharide. Furthermore, the wide temperature range of XG-NH2 from 383 to 700 _C can be observed in Fig. 6. Also, at this stage, the mass loss of XG-NH2 is due to the loss of imine on the material and the degradation of the Xanthan gum base material.35

3.2 Effect of pH on Cu^{2+} removal

pH has a significant effect on the adsorption of metal ions in the adsorption process. To investigate the effect of pH on the removal of Cu2+ by XG-NH2, batch adsorption experiments were conducted at different pH varying from 2 to 6 and the results are shown in Fig. 7. It is clear that the adsorption capacity increases with an increase in pH. At low pH, there is intensive competition between H+ and Cu2+ for adsorption sites because of the high H+ concentration. Obviously, Cu2+ cannot outcompete H+ for biting sites, thus leading to a low adsorption capacity of Cu2+. When the pH is higher than 5, Cu(OH)2 precipitate is formed,36 and precipitation can play a dominant role in the removal of Cu2+ instead of adsorption by XG-NH2. Thus, pH 5 was chosen as the optimum pH to remove Cu2+ from the solutions in the following adsorption experiments. This is in good agreement with the results reported.37

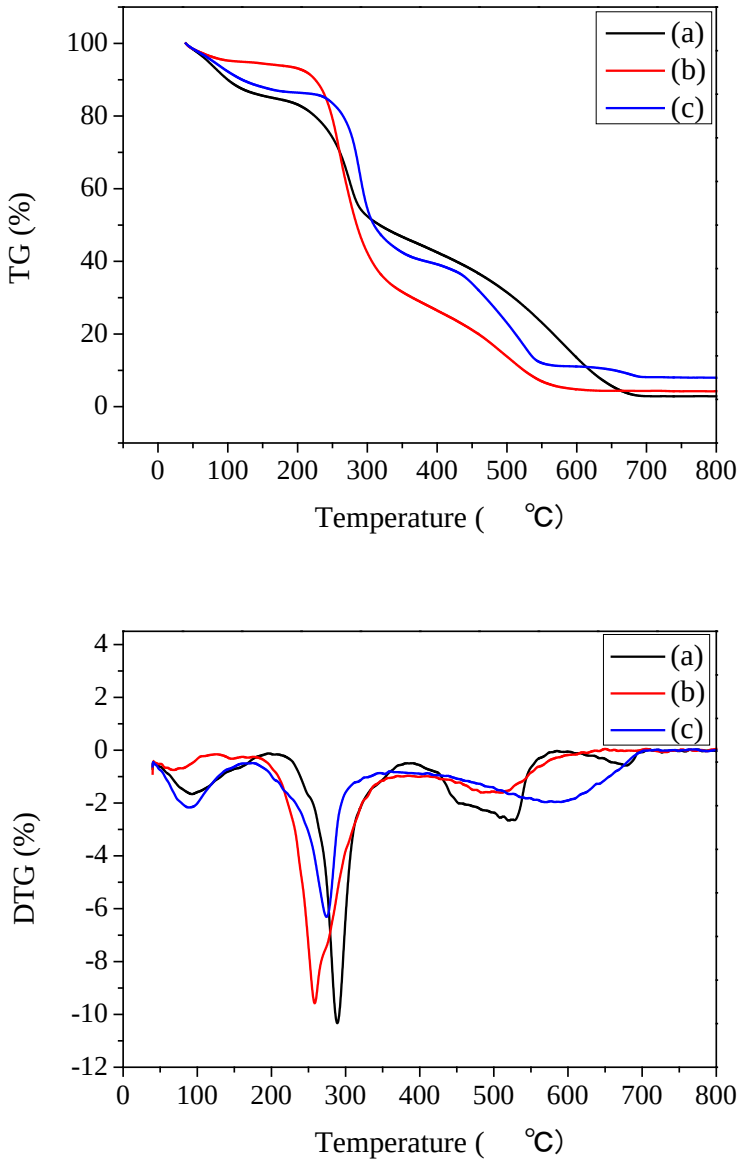

Fig 6 TG/DTG curves of XG(a), XG-Cl(b), XG-NH_2(c).

3.3 Effect of adsorbent dosage

Adsorbent dosage is a significant influencing factor in adsorption experiments. Fig. 8 shows the results of the effect of adsorbent dosage (1 to 5 g L_1) on adsorption of Cu2+. As shown in Fig. 8, the removal rates of Cu2+ increased with an increase in the amount of XG-NH2. This can be ascribed to the increased available adsorption sites to react with Cu2+ with the increase in adsorbent dosage. However, it can be seen from Fig. 8 that the adsorption amount per unit of adsorbent decreases with the increase in dosage of XG-NH2 and this is attributed to the unsaturation of adsorption sites which can be conducive to a decrease in adsorption uptake during the adsorption process.2,38

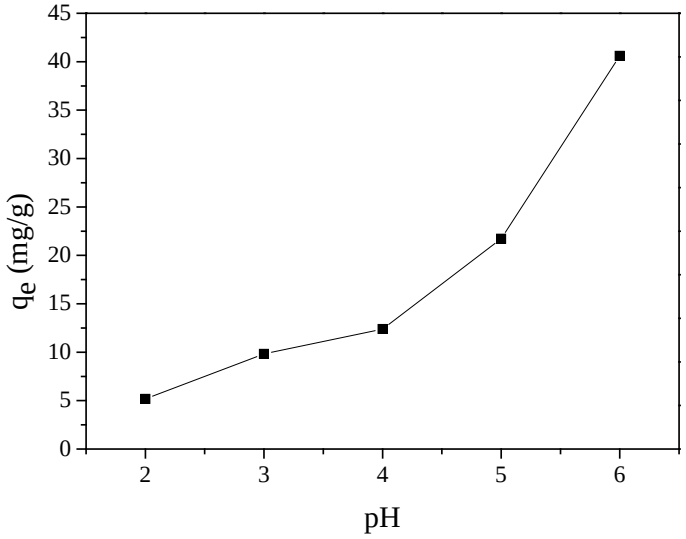

Fig 7 Effect of initial pH on the removal of Cu^{2+}.

3.4 Adsorption Kinetics

Adsorption time is an important factor for the whole adsorption process. As shown in ESI Fig. S2,† the adsorption uptake increased with time and reached a balance at 120 min. Therefore, we chose 120 min as the optimal adsorption time. In order to research adsorption kinetics, the experimental data could be fitted with pseudo-first order, pseudo-second order and intraparticle diffusion kinetic models. The pseudo-first-order kinetic equation21 is expressed as follows:

$$\log(q_e - q_t) = \log q_e - \frac{k_1 t}{2.303} \quad (2)$$

Where q_e and q_t are the amount of Cu2+ adsorbed (mg /g) at equilibrium and at time t, respectively. k_1 is the rate constant of pseudo-first-order adsorption(min-1) .

A linear expression form of pseudo-second order kinetic model is:

$$\frac{t}{q_t} = \frac{1}{k_2 q_e^2} + \frac{t}{q_e} \quad (3)$$

The intra-particle diffusion model equation is (citing reference):

$$q_t = k_p t^{0.5} + C \quad (4)$$

Where k_2 was the equilibrium rate constant of pseudo-second-order adsorption kinetic equation (g mg-1 min-1). k_p was the intra-particle diffusion equation constant (mg h0.5 g-1). C is the intercept gained from the plot of q_t against t0.5.

The experimental results are shown in Fig. S2,† and the corresponding kinetic parameters are summarized in ESI Table S1.† As presented in Fig. S2c,† the kinetic curve was fitted with the pseudosecond- order kinetic equation well. Meanwhile, from Table S1,† we can find that the correlation coefficient of the pseudo-second order kinetic model is

higher than the value of the pseudo-first order model. The calculative equilibrium adsorption capacity (21.50 mg g_1), calculated from the plots of t/qt against t, was close to the experimental adsorption uptake. In Fig. S2d,† it can be seen that the curve of qt against t0.5 is made up of two straight lines, which suggests that the intra-particle diffusion process did not consist of two steps. However, the first straight line did not pass through the origin, which indicates that intra-particle diffusion may not be the rate controlling step.2 Therefore, the adsorption process follows a pseudo-second order kinetic model, which indicates that chemical adsorption was the rate limiting step.39

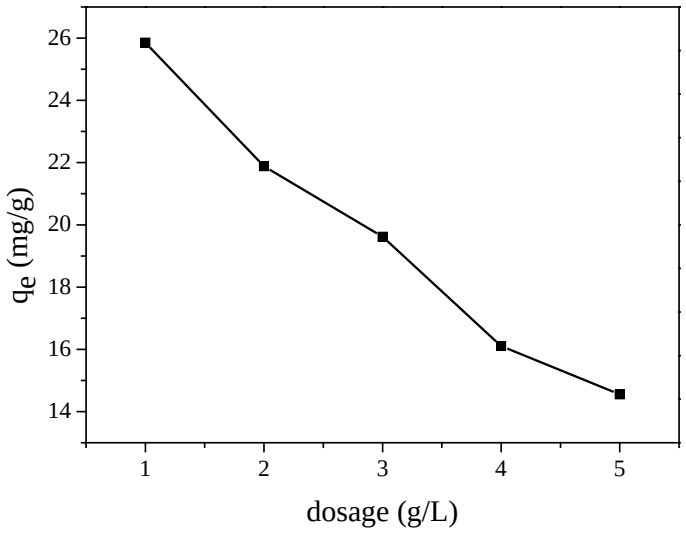

Fig 8 Effect of adsorbent dosage on the removal of Cu^{2+}.

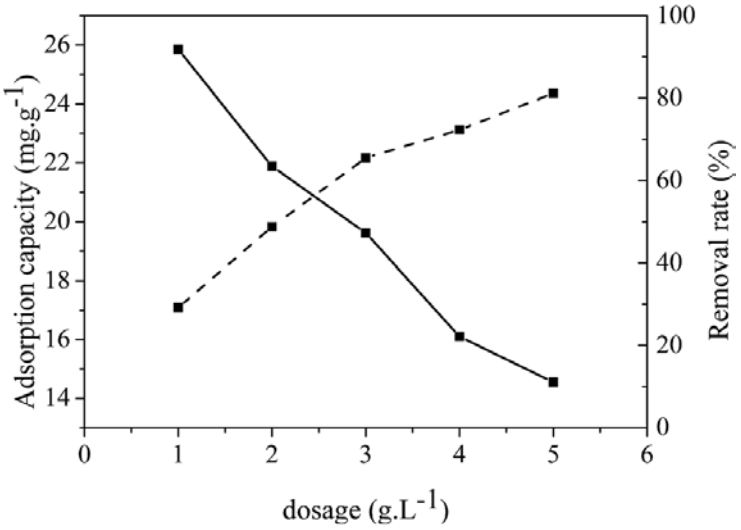

Fig. 9 Effect of adsorbent dosage on the removal of Cu^{2+} (initial concentration, 100 mg L_1; pH, 5; contact time, 2 h at 30 _C, and 250 rpm).

F

3.5 Adsorption Isotherms

Isotherms could be used to illustrate the equilibrium distribution between the adsorbate and solution. In ESI Fig. S3,† the adsorption capacity increased with an increase in the equilibrium concentration firstly and then reached saturation. In order to obtain equilibrium parameters, the Langmuir and Freundlich models are commonly employed to fit the experimental data. The Langmuir isotherm presumes monolayer adsorption according to the assumption of a structurally homogeneous adsorbent where all adsorption sites are assumed to be independent and equivalent. The Langmuir isotherm model40 could be expressed as follows:

$$\frac{C_e}{q_e} = \frac{b}{q_{\max}} + \frac{C_e}{q_{\max}} \quad (5)$$

Where C_e and q_e are the equilibrium concentration (mg/L) and equilibrium adsorption capacity (mg/g), respectively. b and $q_{\max}$ are the Langmuir constant (L/mg) and the maximum adsorption capacity (mg/g), respectively.

The dimensionless adsorption constant (R_L) based on the Langmuir isotherm model can be calculated by the following equation:

$$R_L = \frac{1}{1 + bC_0} \quad (6)$$

The value of reflects that the types of the Langmuir isotherm of unfavorable (> 1), linear (= 1), favorable (0 << 1), or irreversible (= 0).35

The Freundlich isotherm model4, which is still an empirical equation without corresponding assumptions, is represented as:

$$\lg q_e = \lg K_f + \frac{1}{n} \lg C_e \quad (7)$$

Where C_e and q_e are the equilibrium concentration (mg/L) and equilibrium adsorption capacity (mg g-1), respectively. n and K_f (mg/g) are Freundlich adsorption constants.

The experimental data fitted with the Langmuir and Freundlich models are shown in ESI Fig. S3† and their corresponding parameters and respective correlation coefficients are summarized in ESI Table S2.† The results indicate that both the Langmuir and Freundlich models have good linear correlation here, however, the regression coefficients (R2) of the Langmuir model is 0.996, which is higher than the 0.986 of the Freundlich model. This reveals that adsorption process is more suitable for the Langmuir isotherm model due to the higher value of the coefficient compared with the Freundlich model. In addition, the values of RL were smaller than 1, which show that the adsorption process was favorable. According to the Langmuir isotherm, the maximum adsorption capacity of XG-NH2 was approximately 46.95 (mg g_1), which is higher than previous reported adsorbents, such as modified barley straw12 (31.71 mg g_1), modified bagasse pulp cellulose42 (35.2 mg g_1), and amino-functionalized adsorbent36 (33.33 mg g_1). Thus, the modified XG has great potential application as an adsorbent.

3.6 Effect of coexisting salts on Cu^{2+} removal

To investigate the effect of coexisting salts on Cu adsorption by XG-NH2, 0.1 M NaCl, CaCl2, ZnSO4, PbNO3, Ni(NO3)2, Co(NO3)2 and Cd(NO)3 were added to a copper solution, respectively. The results shown in Fig. 9 reveal a slight decreasing trend due to the presence of coexisting ions. This trend indicates that there exists competition between Cu2+ and cations including Na+, Ca2+, Zn2+, Pb2+, Ni2+, Co2+ and Cd2+ for the available binding sites in the adsorption process.

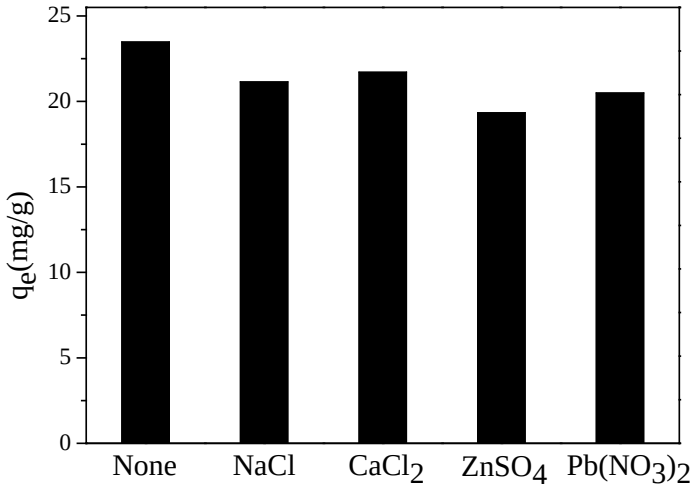

Fig 10 Effect of coexisting salts on the removal of Cu^{2+} .

3.7 Adsorbent Regeneration

To study the regeneration performance of the adsorbent, desorption experiments were carried out with 0.1 M HCl and desorption–adsorption cycles were repeated four times, the results of which are presented in Table 1. With an increase in the cycle numbers, the adsorption capacity decreased significantly, especially after recycling three times. As a consequence, the efficiency of regeneration was low which is attributed to the loss of mass during the washing process and incomplete dissociation of the active sites loaded by copper ions. The regeneration still needs further investigation for improvement.

Table 1 Cyclic adsorption capacity of XG-NH_2 regenerated by 0.1 M HCl.

Cycle number	1	2	3	4
q_e (mg g^{-1})	21.5545	15.9093	9.6819	8.7802

3.8 Comparison with the adsorption effect of different divalent cations

To further investigate the adsorption capacity of different divalent cations by XG-NH2, adsorption experiments for divalent cations (Cu2+, Pb2+, Co2+, Ni2+, Cd2+, Zn2+ and Ca2+) were further performed. The results are summarized in ESI Table S3.† As presented in Table S3,† the adsorption capacities follow the order: Cu2+ > Pb2+ > Cd2+ >Ni2+ > Zn2+ > Co2+ > Ca2+. It can be seen from Table S3† that XG-NH2 has good adsorption capacity for

Cd2+ and Pb2+ except for Cu2+. Therefore, XG-NH2 also can be employed to further remove Cd2+ and Pb2+ from wastewater.

4 Conclusions

In this study, xanthan gum was firstly modified by thionyl chloride, followed by ethylenediamine. Batch xperiments showed that pH, contact time, adsorbent dosage and Cu2+initial concentration have significant influences on the adsorption process. Moreover, the results indicate that coexisting salts have a slight negative effect on the removal of Cu2+. Kinetics studies demonstrate that the process follows a pseudosecond order model with an equilibrium time of 120 min. It was revealed that the rate-limiting stage was chemical adsorption. The Langmuir isotherm and Freundlich model were utilized to fit the experimental data and the Langmuir isotherm had a higher correlation coefficient, hence it was more suitable to describe the isotherm model. The maximum adsorption capacity of Cu2+ was 46.95 mg g_1. The adsorbents loaded by Cu2+ were desorbed with 0.1 M HCl for regeneration. However, the regenerative effect was not ideal after recycling four times. Thus, there are still deficiencies in the adsorbent regeneration and there is broad research value to further improve the regeneration. In addition, the adsorption efficiency of different divalent cations by XG-NH2 indicates that XG-NH2 has potential for the further adsorption of Cd2+ and Pb2+.

Acknowledgements

This work was supported by Open Fund (PLN1134) of State Key Laboratory of Oil Gas Reservoir Geology and Exploitation (Southwest Petroleum University) of China. The authors express their thanks to the Open Fund.

References

1 Y. Dong and H. Lin, Trans. Nonferrous Met. Soc. China, 2015, 25, 991–996.

2 J. Gong, X. Wang, G. Zeng, L. Chen, J. Deng, X. Zhang and Q. Niu, Chem. Eng. J., 2012, 185–186, 100–107.

3 P. K. Ingle, C. Gadipelly and V. K. Rathod, Desalin. Water Treat., 2015, 55, 401–409.

4 Y. Yu, J. G. Shapter, R. Popelka-Filcoff, J. W. Bennett and A. V. Ellis, J. Hazard. Mater., 2014, 273, 174–182.

5 N. Chiron, R. Guilet and E. Deydier, Water Res., 2003, 37, 3079–3086.

6 K. Li, Y. Wang, M. Huang, H. Yan, H. Yang, S. Xiao and A. M. Li, J. Colloid Interface Sci., 2015, 455, 261–270.

7 X. Lu, P. Yan and X. Dang, Adv. Mater. Res., 2013, 864–867, 1327–1332.

8 Y. N. Mata, M. L. Bl´azquez, A. Ballester, F. Gonz´alez and J. A. Mu˜noz, Chem. Eng. J., 2009, 150, 289–301.

9 B. Zhao, W. Peng, Z. Tong, C. Chun and S. Jing, J. Appl. Polym. Sci., 2006, 99, 2951–2956.

10 S. Liang, X. Guo, N. Feng and Q. Tian, J. Hazard. Mater., 2010, 174, 756–762.

11 T. S. Anirudhan and S. Rijith, Colloids Surf., A, 2009, 351, 52– 59.

12 E. Pehlivan, T. Altun and S. Parlayici, Food Chem., 2012, 135, 2229–2234.

13 A. Mart´ınez-Ruvalcaba, E. Chornet and D. Rodrigue, Carbohydr. Polym., 2007, 67, 586–595.

14 D. F. S. Petri, J. Appl. Polym. Sci., 2015, 132, 1–13.

15 D. Bergmann, G. Furth and C. Mayer, Int. J. Biol. Macromol., 2008, 43, 245–251.

16 E. A. Elizalde-Pena, D. G. Zarate-Trivino, S. M. Nuno- Donlucas, L. Medina-Torres, J. E. Gough, I. C. Sanchez, F. Villasenor and G. Luna-Barcenas, J. Biomater. Sci., Polym. Ed., 2013, 24, 1426–1442.

17 I. Nor Hayati, C. Wai Ching and M. Z. H. Rozaini, Food Hydrocolloids, 2016, 53, 199–208.

18 Y. Tao, R. Zhang, W. Xu, Z. Bai, Y. Zhou, S. Zhao, Y. Xu and D. Yu, Food Hydrocolloids, 2016, 52, 923–933.

19 S. Ghorai, A. Sinhamahpatra, A. Sarkar, A. B. Panda and S. Pal, Bioresour. Technol., 2012, 119, 181–190.

20 X. Peng, F. Xu, W. Zhang, J. Wang, C. Zeng, M. Niu and E. Chmielewsk´a, Colloids Surf., A, 2014, 443, 27–36.

21 W. Zhang, F. Xu, Y. Wang, M. Luo and D. Wang, Chem. Eng. J., 2014, 255, 316–326.

22 A. R. Cestari, E. F. Vieira, A. J. Nascimento, F. J. de Oliveira, R. E. Bruns and C. Airoldi, J. Colloid Interface Sci., 2001, 241, 45–51.
23 L. V. A. Gurgel and L. F. Gil, Carbohydr. Polym., 2009, 77, 142– 149.
24 V. S. O. Ruiz, G. C. Petrucelli and C. Airoldi, J. Mater. Chem., 2006, 16, 2238–2346.
25 E. C. da Silva Filho, L. S. da Silva, L. C. B. Lima, L. D. S. Santos J´unior, M. R. D. M. C. Santos, J. M. E. de Matos and C. Airoldi, Sep. Sci. Technol., 2011, 46, 2566–2574.
26 E. C. da Silva Filho, S. A. A. Santana, J. C. P. Melo, F. J. V. E. Oliveira and C. Airoldi, J. Therm. Anal. Calorim., 2010, 100, 313–325.
27 E. C. da Silva Filho, J. C. de Melo and C. Airoldi, Carbohydr. Res., 2006, 341, 2842–2850.
28 S. M. Musyoka, J. C. Ngila, B. Moodley, L. Petrik and A. Kindness, Anal. Lett., 2011, 44, 1925–1936.
29 J. Chen, J. Feng and W. Yan, RSC Adv., 2015, 5, 86945–86953.
30 Y. Li, B. Zhao, L. Zhang and R. Han, Desalin. Water Treat., 2013, 51, 5735–5745.
31 C. Y. Lii, S. C. Liaw and P. Tomasik, Pol. J. Food Nutr. Sci., 2003, 53, 25–29.
32 A. M. S. Maia, H. V. M. Silva, P. S. Curti and R. C. B. Balaban, Carbohydr. Polym., 2012, 90, 778–783.
33 Y. Wang, C. Li, P. Liu, Z. Ahmed, P. Xiao and X. Bai, Carbohydr. Polym., 2010, 82, 895–903.
34 K. Behari, P. K. Pandey, R. Kumar and K. Taunk, Carbohydr. Polym., 2001, 46, 185–189.
35 D. A. da Silva, R. C. M. de Paula and J. P. A. Feitosa, Eur. Polym. J., 2007, 43, 2620–2629.
36 W. Peng, Z. Xie, G. Cheng, L. Shi and Y. Zhang, J. Hazard. Mater., 2015, 294, 9–16.
37 B. Zhu, T. Fan and D. Zhang, J. Hazard. Mater., 2008, 153, 300–308.
38 Z. Wang, P. Han, Y. Jiao, D. Ma, C. Dou and R. Han, Desalin. Water Treat., 2012, 30, 195–206.
39 A. Sharma and B.-K. Lee, Appl. Surf. Sci., 2014, 313, 624–632.
40 G. Lan, X. Hong, Q. Fan, B. Luo, P. Shi and X. Chen, J. Appl. Polym. Sci., 2014, 131, 1–11.
41 V. de Oliveira Sousa Neto, D. Q. Melo, T. C. de Oliveira, R. N. P. Teixeira, M. A. A. ujo Silva and R. F. do Nascimento, Appl. Polym. Sci., 2014, 131, 1–11.
42 H. Zhu, X. Cao, Y. He, Q. Kong, H. He and J. Wang, Carbohydr. Polym., 2015, 129, 115–126.